Higgs-flavon mixing and h -> mu tau

Huitu, Katri

2016-05-04

Higgs-flavon mixing and $h \to \mu\tau$

Katri Huitu, Venus Keus, Niko Koivunen and Oleg Lebedev

Department of Physics and Helsinki Institute of Physics,
Gustaf Hällströmin katu 2, FIN-00014 University of Helsinki, Finland

E-mail: Katri.Huitu@helsinki.fi, Venus.Keus@helsinki.fi,
Niko.Koivunen@helsinki.fi, Oleg.Lebedev@helsinki.fi

Abstract: ATLAS and CMS have reported an excess in the flavor violating decay of the Higgs boson, $h \to \mu\tau$. We show that this result can be accommodated through a mixing of the Higgs with a flavon, the field responsible for generating the Yukawa matrices in the lepton sector. We employ a version of the Froggatt-Nielsen mechanism at the electroweak scale, with only the leptons and the flavon transforming non-trivially under the corresponding symmetry group. Non-observation of charged lepton flavor violation (LFV) in other processes imposes important constraints on the model, which we find to be satisfied in substantial regions of parameter space.

Contents

1 Introduction

In the Standard Model (SM), the fermion Yukawa couplings are free parameters with no explanation for the hierarchy among the fermion masses spanning over six orders of magnitude. Several Beyond the Standard Model (BSM) scenarios have been proposed to resolve this puzzle. A popular BSM framework was suggested by Froggatt and Nielsen developing a mechanism that naturally generates the SM fermion Yukawa couplings [1].

Lepton Flavour Violating (LFV) processes are absent in the SM, which has been consistent with observations. Yet, recently the CMS and ATLAS experiments have hinted at the existence of a flavour violating decay of the Higgs boson $h \to \mu\tau$ [2, 3].[1] The combined branching ratio for this decay is found to be

$$\mathrm{BR}(h \to \mu\tau) = 0.82^{+0.33}_{-0.32} \, \% \,, \tag{1.1}$$

while it is zero in the SM. In this paper, we study the possibility that this observation is due to a mixing between the SM Higgs field and a *flavon*, which is an integral part of the Froggatt-Nielsen mechanism [1]. The latter requires the existence of a scalar field (flavon) charged under an extra U(1)-symmetry which is broken spontaneously by its Vacuum Expectation Value (VEV). The usual Higgs-portal [4–6] coupling between the Higgs and the flavon field then leads to the Higgs-flavon mixing or, in other words, the existence of two mass eigenstates H_1 and H_2. The lighter state, H_1, is identified with the 125 GeV Higgs-like scalar h observed at the LHC, while the heavier state, H_2, has a dominant flavon component. Both of these scalars possess flavor changing couplings due to a misalignment between the lepton mass matrix and the matrix of the scalar couplings (see also [7–9]).

---

[1]The process $h \to l_i l_j$ includes both $h \to l_i^+ l_j^-$ and $h \to l_i^- l_j^+$.

To avoid the appearance of a Goldstone boson, the Froggatt-Nielsen symmetry should be gauged, discrete or softly broken. We find that the gauge symmetry option is strongly constrained and does not lead to a substantial BR($h \to \mu\tau$). On the other hand, the discrete and softly broken versions of the Froggatt-Nielsen mechanism can be viable. In this work, we focus on the *leptophilic* flavon which generates flavor structures in the lepton sector only, while the quark sector may possess its own flavon(s). In this case, the quark flavor changing processes do not constrain our model.

Lepton flavor violation induced by the Standard Model Higgs has been the subject of intense research in recent years, starting with ref. [10] where it was found that the low energy LFV constraints in the (μ, τ) sector are quite weak. Ref. [11] observed that a large $h \to \mu\tau$ rate comparable to that of $h \to \tau\tau$ is consistent with these bounds. This idea received a boost from experiment when the tentative signal (1.1) was detected which was followed by a surge in theory constructions. Relevant analyses of Higgs-induced lepton flavor violation include refs. [12]–[30]. Our approach here differs from previous work in a few aspects. In particular, we treat leptons and quarks on a different basis, which allows for the electroweak scale flavon sector. We also observe that the LFV processes in the Froggatt-Nielsen framework are subject to certain natural cancellations.

The remainder of this paper is organized as follows. In section 2, we introduce our Froggatt-Nielsen set-up. In section 3, we choose a favorable Yukawa texture and study all the relevant LFV constraints. The Higgs decay into leptons is analyzed in section 4, where we also provide an example of the parameter region saturating the experimental result (1.1). We conclude in section 5.

2 The Froggatt-Nielsen framework

The salient feature of the Froggatt-Nielsen mechanism is that the SM Yukawa interactions are generated through higher dimensional operators consistent with some U(1) symmetry and the resulting Yukawa matrix is given in terms of the VEV of the flavon Φ,

$$c_{ij} \frac{\Phi^{n_{ij}}}{\Lambda^{n_{ij}}} \bar{f}_{L,i} f_{R,j} H + \text{h.c.} \,, \tag{2.1}$$

where c_{ij} are order one coefficients, Λ is the new physics scale and $f_{L,R}$ are SM fermions. Such operators are obtained by integrating out heavy states at the scale Λ. When Φ develops a VEV,

$$\Phi = \frac{1}{\sqrt{2}}(v_\phi + \phi) \tag{2.2}$$

with $\phi = \text{Re}\phi + i\text{Im}\phi$, the Yukawa couplings are given by

$$Y_{ij} = c_{ij} \left(\frac{v_\phi}{\sqrt{2}\Lambda}\right)^{n_{ij}} \equiv c_{ij} \, \epsilon^{n_{ij}} \,, \tag{2.3}$$

where ϵ is a small parameter. The U(1) invariance of the operator (2.1) requires

$$n_{ij} = -\frac{1}{q_\phi}(q_{\bar{L},i} + q_{R,j} + q_h) \,, \tag{2.4}$$

Particle	$f^c_{L,i}$	$f_{R,i}$	H	Φ
U(1) charge	$q_{\bar{L},i}$	$q_{R,i}$	q_h	q_ϕ

Table 1. The U(1) charges of SM fermions $f_{R,L}$, SM Higgs field H and the flavon Φ.

where q_i are the charges identified in table 1. The main attractive feature of the Froggatt-Nielsen mechanism is that order one charges translate into a hierarchy among the Yukawa couplings, thereby eliminating unnaturally small dimensionless parameters from the flavour sector.

In addition to the SM Yukawa couplings, integrating out heavy particles induces further operators, e.g.

$$\left(\frac{\Phi}{\Lambda}\right)^{l_{ij}} \bar{f}_{L,i}\,\slashed{\partial}f_{L,j}\ ,\ \ \partial_\mu \left(\frac{\Phi}{\Lambda}\right)^{l_{ij}} \bar{f}_{L,i}\gamma^\mu f_{L,j}, \tag{2.5}$$

where l_{ij} is some combination of charges, and similarly for the right-handed fermions. Here it is understood that if $l_{ij} < 0$, the flavon is to be replaced by its complex conjugate, $\Phi^{l_{ij}} \to (\Phi^*)^{-l_{ij}}$. For $\Phi/\Lambda \ll 1$, the fermion kinetic terms can be diagonalized by a Φ-dependent field redefinition, which also induces operators of the second type in (2.5). Due to U(1)-invariance the Yukawa textures (2.3) are not affected by this transformation, while the order one coefficients can change.[2] Further, in the new basis the interaction terms involving $\partial_\mu \Phi$ can be rewritten as the Yukawa terms using the fermion equations of motion. Therefore, the ϵ-dependence of the ϕ-couplings is not affected by such manipulations and we shall focus entirely on the Yukawa operator (2.1).

In this work, we will only consider the lepton sector. This is sufficient if only the leptons and the flavon transform under the (leptonic) U(1) symmetry, while the quark sector enjoys a different symmetry group. As the Higgs field develops a VEV,

$$H = \begin{pmatrix} 0 \\ \frac{v+h}{\sqrt{2}} \end{pmatrix}, \tag{2.6}$$

the effective interaction involving the leptons and no more than one physical scalar takes the form

$$\mathcal{L}_{\text{eff}} \supset \frac{v}{\sqrt{2}}\, Y_{ij}\, \left(1 + \frac{h}{v} + n_{ij}\,\frac{\phi}{v_\phi}\right) \bar{l}'_{L,i} l'_{R,j}\ . \tag{2.7}$$

Here, the prime in the lepton fields serves to distinguish the weak basis (l') from the mass eigenstate basis (l). We see that while the Higgs interactions have the same flavour structure as the Yukawa matrices, those of the flavon do not which leads to flavour changing vertices.

Redefining the left-handed and right-handed leptons, one can diagonalize the lepton mass matrix. With

$$Y_{\text{diag}} = U_L Y U_R^\dagger, \tag{2.8}$$

---

[2]This may also induce higher order corrections involving powers of $\Phi^*\Phi/\Lambda^2$.

where $U_{L,R}$ are unitary matrices, we get the following interactions in the mass eigenstate basis:

$$\mathcal{L}_{\text{eff}} \supset \bar{l}_L \, M_{\text{diag}} \, l_R + \frac{h}{\sqrt{2}} \, \bar{l}_L \, Y_{\text{diag}} \, l_R + \frac{\phi}{\sqrt{2}} \frac{v}{v_\phi} \, \bar{l}_L \, \kappa \, l_R + \text{h.c.}, \tag{2.9}$$

where $M_{\text{diag}} = Y_{\text{diag}} v / \sqrt{2}$ and the flavon vertex involves the matrix

$$\kappa = U_L \, (Y \cdot n) \, U_R^\dagger, \tag{2.10}$$

with $(Y \cdot n)_{ij} \equiv Y_{ij} n_{ij}$. Since $n_{ij} = a_i + b_j$, the matrix $Y \cdot n$ can be expressed in terms of a matrix product which allows us to write κ in a closed form. Setting

$$q_\Phi = -1 \ , \quad q_h = 0 \tag{2.11}$$

throughout this paper, we have

$$\kappa_{ij} = y_j \sum_{k=1}^{3} q_{\bar{L},k}(U_L)_{ik}(U_L)_{jk}^* + y_i \sum_{k=1}^{3} q_{R,k}(U_R)_{ik}(U_R)_{jk}^*, \tag{2.12}$$

where y_i are the Yukawa matrix eigenvalues. This is the source of lepton flavor violation in our model. Upon the Higgs-flavon mixing, such flavor changing couplings also appear in the interactions of the physical Higgs-like boson.

It is important to note that the neutrino sector does not have a direct impact on our considerations. Indeed, the LFV couplings are due to the matrices $U_{L,R}$ which diagonalize the charged lepton mass matrix. Here we simply assume that realistic neutrino textures can be generated by some mechanism which depends on the nature of the right-handed neutrinos and their multiplicity.[3]

Let us now turn to the scalar sector of the model. The U(1)-symmetric scalar potential is given by

$$V(H, \Phi) = -\mu_h^2(H^\dagger H) + \lambda_h(H^\dagger H)^2 - \mu_\phi^2(\Phi^\dagger \Phi) + \lambda_\phi(\Phi^\dagger \Phi)^2 + \lambda_{h\phi}(H^\dagger H)(\Phi^\dagger \Phi) \ . \tag{2.13}$$

At the minimum of the potential, both H and Φ develop VEVs leading to a mixing between h and $\text{Re}\phi$ (assuming CP invariance),

$$\begin{pmatrix} H_1 \\ H_2 \end{pmatrix} \equiv \begin{pmatrix} \cos\theta & \sin\theta \\ -\sin\theta & \cos\theta \end{pmatrix} \begin{pmatrix} h \\ \text{Re}\phi \end{pmatrix}. \tag{2.14}$$

The explicit form of θ and the $H_{1,2}$ masses in terms of the parameters of the potential is not needed for our purposes and can be found elsewhere (see e.g. [32]). We take the lighter boson H_1 to be the 125 GeV Higgs-like scalar observed at the LHC and parametrize our results in terms of θ and m_{H_2}. These are constrained by the collider data, most importantly, by the LHC and the electroweak precision measurements as summarized in [33].

Since the vacuum breaks the Froggatt-Nielsen symmetry, a global U(1) would result in a massless Goldstone boson which is phenomenologically unacceptable. There are a few

---

[3]The number of right-handed neutrinos can in principle be very large [31].

ways to circumvent this problem. One may gauge the U(1), however we find that this option does not lead to interesting phenomenology due to tight constraints on a flavor non-universal Z'. More interesting possibilities include discretizing the U(1) → Z_N or introducing a soft explicit breaking. In the Z_N case, one can add to the Lagrangian the operator

$$\frac{c}{\Lambda^{N-4}} \, \Phi^N + \text{h.c.} \, , \tag{2.15}$$

which generates $m_{\text{Im}\phi}$ of order $\sqrt{c}v_\phi(v_\phi/\Lambda)^{N/2-2}$. Models with large $N \sim 10$ then include a rather light pseudoscalar (unless c is large). In the case of soft explicit U(1) breaking, one includes

$$\tilde{m}^2\Phi^2 + \text{h.c.} \, , \tag{2.16}$$

which induces $m_{\text{Im}\phi} \sim \tilde{m}$. In more involved models, such a mass term can also result from a VEV of another scalar which does not couple to the SM fermions and thus does not alter the Yukawa textures. In what follows, we will be agnostic as to the origin of the Imϕ mass and will simply parametrize our results in terms of $m_{\text{Im}\phi}$.

Finally, it is important to keep in mind the limitations of our effective field theory approach. While tree level processes are well under control, the loop contributions in our framework are only indicative in nature since they depend on the details of the UV completion. This issue can be addressed in specific models whereas here we provide the expected lower limit on loop induced LFV.

3 Bounds on flavon-induced lepton flavor violation

The flavon interaction (2.9) induces lepton flavor violating processes which are strongly constrained by experiment. In this section, we derive the corresponding limits on the flavon couplings parametrized by

$$\tilde{\kappa}_{ij} = \frac{1}{\sqrt{2}} \frac{v}{v_\phi} \kappa_{ij} \, , \tag{3.1}$$

such that the flavon-lepton coupling is $\tilde{\kappa}_{ij} \, \bar{l}_{L,i} \, l_{R,j}\phi+$ h.c. In our analysis, we use the current bounds from the three-body decay $l_i \to l_j l_k l_l$, magnetic transition $l_i \to l_j\gamma$ and $\mu \to e$ conversion processes presented in table 2.

Throughout the paper we use a specific Yukawa texture which, as we show later, induces interesting LFV effects in Higgs decay and accommodates the $h \to \mu\tau$ result. Omitting for simplicity possible CP phases, the charge assignment shown in table 3 leads to

$$Y = \begin{pmatrix} 3.4 \, \epsilon^6 & -0.6 \, \epsilon^6 & 3.5 \, \epsilon^7 \\ 5.4 \, \epsilon^4 & 6.1 \, \epsilon^4 & -3.1 \, \epsilon^5 \\ 0.5 \, \epsilon^2 & 0.5 \, \epsilon^2 & 7.3 \, \epsilon^3 \end{pmatrix}, \quad \tilde{\kappa} = \frac{v}{v_\phi} \begin{pmatrix} 1 \times 10^{-5} & -1 \times 10^{-6} & -3 \times 10^{-6} \\ -2 \times 10^{-5} & 2 \times 10^{-3} & 6 \times 10^{-4} \\ 3 \times 10^{-4} & -4 \times 10^{-3} & 2 \times 10^{-2} \end{pmatrix},$$

which reproduces the correct lepton masses for $\epsilon = 0.1$ and the shown proportionality coefficients (their precise values are given in appendix A). The key feature here is that the Yukawa matrix is far from diagonal, leading to a large $\mu - \tau$ mixing. Other possible textures will be explored in our subsequent work.

	Observable	Present limit
1	$\mathrm{BR}(\mu \to eee)$	1.0×10^{-12} [34]
2	$\mathrm{BR}(\tau \to eee)$	3.0×10^{-8} [35]
3	$\mathrm{BR}(\tau \to \mu\mu\mu)$	2.0×10^{-8} [35]
4	$\mathrm{BR}(\tau^- \to \mu^- e^+ e^-)$	1.7×10^{-8} [36]
5	$\mathrm{BR}(\tau^- \to e^- \mu^+ \mu^-)$	2.7×10^{-8} [36]
6	$\mathrm{BR}(\tau^- \to e^+ \mu^- \mu^-)$	1.7×10^{-8} [36]
7	$\mathrm{BR}(\tau^- \to \mu^+ e^- e^-)$	1.5×10^{-8} [36]
8	$\mathrm{BR}(\mu \to e\gamma)$	5.7×10^{-13} [37]
9	$\mathrm{BR}(\tau \to \mu\gamma)$	4.4×10^{-8} [35]
10	$\mathrm{BR}(\tau \to e\gamma)$	3.3×10^{-8} [35]
11	$\mathrm{CR}(\mu\text{-}e, Au)$	7.0×10^{-13} [38]

Table 2. Current experimental bounds on the branching ratios of three-body LFV decays, magnetic transitions and the conversion rate of $\mu \to e$.

Particle	e_L^c	e_R	μ_L^c	μ_R	τ_L^c	τ_R	H	ϕ
Charge	6	0	4	0	2	1	0	-1

Table 3. U(1)/Z_N charge assignment.

In the discrete symmetry case, Z_N acts on a given field by multiplying it with $e^{2\pi q_i i/N}$ where N is the order of Z_N and q_i is the corresponding charge from table 3. In the allowed couplings the charges add up to zero mod N. The Yukawa texture then has the above form for $N \geq 14$.[4] Our LFV results equally apply to this case as well.

Given the texture, we can now derive bounds on the flavon VEV and mass. If our U(1) is gauged, the flavon VEV has to be very large and no interesting effects in Higgs decay are expected. This can be seen, for instance, from the corresponding Z' contribution to $\mu \to eee$. Since the gauge coupling factors cancel between the vertices and the propagator, this process probes v_ϕ directly:

$$\frac{\Gamma(\mu \to eee)}{\Gamma(\mu \to e\nu\bar{\nu})}\bigg|_{Z'} \sim \frac{v^4}{v_\phi^4} \, \sin^2\delta_{e\mu} < \mathcal{O}(10^{-12}) \,, \tag{3.2}$$

where $\delta_{e\mu}$ is the mixing angle appearing at the $Z'\bar{e}\mu$-vertex. For the textures we consider, v_ϕ has to be at least $\mathcal{O}(10\,\mathrm{TeV})$, which makes $\tilde{\kappa}$ negligibly small.

In what follows, we therefore focus on the global symmetry case, which implies in particular that $\mathrm{Im}\phi$ is a physical degree of freedom. The diagrams which contribute to the LFV observables depend in general on the Higgs-flavon mixing. We thus consider in detail two cases: (i) negligible Higgs-flavon mixing, (ii) substantial Higgs-flavon mixing.

---

[4]For smaller N, one can get allowed couplings at lower order in ϵ by replacing Φ with Φ^*.
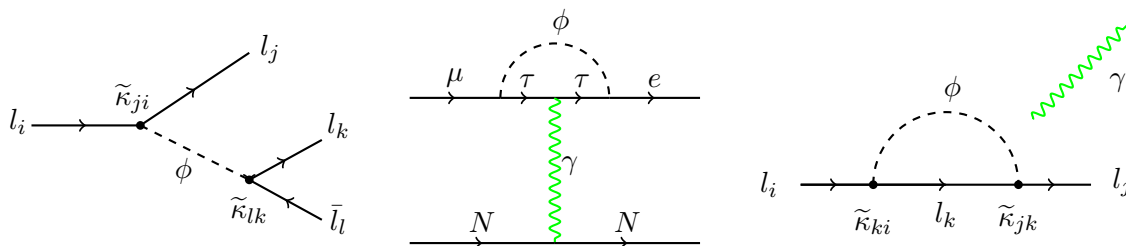
Figure 1. The $l_i \to l_j l_k l_l$ (left), $\mu \leftrightarrow e$-conversion (center) and $l_i \to l_j \gamma$ (right) processes mediated by the flavon ϕ. The decay $l_i \to l_j l_k l_l$ also receives important contributions at one loop.

3.1 Negligible Higgs-flavon mixing

When the Higgs-flavon mixing is close to zero, all lepton flavor violation is due to the exchange of $\mathrm{Re}\phi$ and $\mathrm{Im}\phi$, which are mass eigenstates. This limiting case is instructive to consider and easy to generalize to a more interesting scenario with a non-zero mixing. To make the discussion more transparent we decouple $\mathrm{Im}\phi$ in this subsection ($m_{\mathrm{Im}\phi} \to \infty$), whereas in the more realistic case of a non-zero mixing we take it properly into account.

We start by studying the 3-body decays $l_i \to l_j l_j l_j$ (figure 1, left). These receive contributions both at tree level and 1-loop. The latter, with the photon attached to $l_j^+ l_j^-$, can be important since they involve a tau in the loop whose coupling is enhanced by the tau mass. The total decay rate for a given process is $\Gamma_{\mathrm{tot}} = \Gamma^{\mathrm{tree}} + \Gamma^{1-\mathrm{loop}}$. Due to the different helicity structures, the tree and loop amplitudes do not interfere. We find for the most important processes[5]

$$\Gamma^{\mathrm{tree}}(l_i \to l_j l_j l_j) = \frac{m_i^5}{4096\pi^3} \frac{(|\widetilde{\kappa}_{ji}|^2 + |\widetilde{\kappa}_{ij}|^2)|\widetilde{\kappa}_{jj}|^2}{m_{\mathrm{Re}\phi}^4} , \tag{3.3}$$

$$\Gamma^{1-\mathrm{loop}}(\mu \to eee) = \frac{\alpha^2 m_\mu^3 m_\tau^2}{3072\pi^5} \frac{|\widetilde{\kappa}_{\tau e}|^2 |\widetilde{\kappa}_{\mu\tau}|^2 + |\widetilde{\kappa}_{e\tau}|^2 |\widetilde{\kappa}_{\tau\mu}|^2}{m_{\mathrm{Re}\phi}^4} \left[\frac{3}{2} - \log\left(\frac{m_{\mathrm{Re}\phi}^2}{m_\tau^2}\right) \right]^2 \left[\log\left(\frac{m_\mu^2}{m_e^2}\right) - \frac{11}{4} \right],$$

$$\Gamma^{1-\mathrm{loop}}(\tau \to \mu\mu\mu) = \frac{\alpha^2 m_\tau^5}{3072\pi^5} \frac{(|\widetilde{\kappa}_{\tau\mu}|^2 + |\widetilde{\kappa}_{\mu\tau}|^2)|\widetilde{\kappa}_{\tau\tau}|^2}{m_{\mathrm{Re}\phi}^4} \left[\frac{4}{3} - \log\left(\frac{m_{\mathrm{Re}\phi}^2}{m_\tau^2}\right) \right]^2 \left[\log\left(\frac{m_\tau^2}{m_\mu^2}\right) - \frac{11}{4} \right],$$

and analogously for $\Gamma^{1-\mathrm{loop}}(\tau \to eee)$.

The radiative transitions $l_i \to l_j \gamma$ (figure 1, right) typically impose the strongest constraints on LFV models. In our case, the diagrams with the tau in the loop dominate. Neglecting the light lepton contributions, we find

$$\Gamma(\mu \to e\gamma) = \frac{\alpha m_\mu^3 m_\tau^2}{1024\pi^4} \frac{|\widetilde{\kappa}_{e\tau}|^2 |\widetilde{\kappa}_{\tau\mu}|^2 + |\widetilde{\kappa}_{\tau e}|^2 |\widetilde{\kappa}_{\mu\tau}|^2}{m_{\mathrm{Re}\phi}^4} \left[\frac{3}{2} - \log\left(\frac{m_{\mathrm{Re}\phi}^2}{m_\tau^2}\right) \right]^2 , \tag{3.4}$$

$$\Gamma(\tau \to \mu\gamma) = \frac{\alpha m_\tau^5}{1024\pi^4} \frac{(|\widetilde{\kappa}_{\mu\tau}|^2 + |\widetilde{\kappa}_{\tau\mu}|^2)|\widetilde{\kappa}_{\tau\tau}|^2}{m_{\mathrm{Re}\phi}^4} \left[\frac{4}{3} - \log\left(\frac{m_{\mathrm{Re}\phi}^2}{m_\tau^2}\right) \right]^2 .$$

An analogous expression holds for $\Gamma(\tau \to e\gamma)$ as well.

------

[5]These results agree with those of ref. [39].

Observable	Constraint
$\mathrm{BR}(\mu^- \to e^- e^- e^+)$	$|\widetilde{\kappa}_{\tau e}|\, |\widetilde{\kappa}_{\mu\tau}| < 7.6 \times 10^{-6}$
$\mathrm{BR}(\tau^- \to e^- e^- e^+)$	$|\widetilde{\kappa}_{\tau e}|\, |\widetilde{\kappa}_{\tau\tau}| < 3.8 \times 10^{-3}$
$\mathrm{BR}(\tau^- \to \mu^- \mu^- \mu^+)$	$|\widetilde{\kappa}_{\mu\tau}|\, |\widetilde{\kappa}_{\mu\mu}| < 3.1 \times 10^{-3}$
$\mathrm{BR}(\mu \to e\gamma)$	$|\widetilde{\kappa}_{e\tau}|\, |\widetilde{\kappa}_{\tau\mu}| < 4.5 \times 10^{-7}$
$\mathrm{BR}(\tau \to \mu\gamma)$	$|\widetilde{\kappa}_{\tau\mu}|\, |\widetilde{\kappa}_{\tau\tau}| < 4.9 \times 10^{-3}$
$\mathrm{BR}(\tau \to e\gamma)$	$|\widetilde{\kappa}_{\tau e}|\, |\widetilde{\kappa}_{\tau\tau}| < 4.2 \times 10^{-3}$

Table 4. Strongest bounds on the LFV couplings for a symmetric $\widetilde{\kappa}$-texture and $m_{\mathrm{Re}\phi} = 500\,\mathrm{GeV}$. For other flavon masses, the bounds rescale approximately by $(m_{\mathrm{Re}\phi}/500\,\mathrm{GeV})^2$.

Finally, we also include constraints from the $\mu \leftrightarrow e$ conversion (figure 1, center). Since the flavon does not couple to quarks, it is a loop process mediated by a tau. The conversion rate is

$$\Gamma(\mu \leftrightarrow e) = \left| \frac{iD}{2m_\mu} A^L_{\mu \to e\gamma} + \widetilde{g}^{(p)}_{LV} V^{(p)} \right|^2 + \left| \frac{iD}{2m_\mu} A^R_{\mu \to e\gamma} + \widetilde{g}^{(p)}_{RV} V^{(p)} \right|^2, \tag{3.5}$$

where we use $\Gamma_{\mathrm{capture}\ Au} = 13.07 \times 10^6 s^{-1}$, and D and $V^{(p)}$ are the overlap integrals for the nucleus in question. For gold, these integrals are [40] $D = 0.189$ and $V = 0.0974$ in units of $m_\mu^{5/2}$. Here the same distribution is assumed for neutrons and protons in the nucleus [41]. The Wilson coefficients are

$$\widetilde{g}^{(p)}_{LV} = \frac{\alpha}{6\pi} \frac{\widetilde{\kappa}_{e\tau} \widetilde{\kappa}^*_{\mu\tau}}{m^2_{\mathrm{Re}\phi}} \left[-\frac{11}{6} + \log\left(\frac{m^2_{\mathrm{Re}\phi}}{m^2_\tau}\right) \right], \tag{3.6}$$

and $\widetilde{g}^{(p)}_{RV}$ is obtained from $\widetilde{g}^{(p)}_{LV}$ by replacing $\widetilde{\kappa}_{ij}$ with $\widetilde{\kappa}^*_{ji}$. The invariant amplitude $A^L_{\mu \to e\gamma}$ is

$$A^L_{\mu \to e\gamma} = -\frac{ie}{32\pi^2} \widetilde{\kappa}^*_{\tau e} \widetilde{\kappa}^*_{\mu\tau} \left[\frac{3}{2} - \log\left(\frac{m^2_{\mathrm{Re}\phi}}{m^2_\tau}\right) \right] \frac{m_\tau}{m^2_{\mathrm{Re}\phi}} . \tag{3.7}$$

The corresponding expression for A^R is obtained by replacing $\widetilde{\kappa}_{ij}$ with $\widetilde{\kappa}^*_{ji}$.

To illustrate the strength of the constraints, in table 4 we present a summary of the resulting bounds on $\tilde{\kappa}_{ij}$ assuming a *symmetric* $\tilde{\kappa}_{ij}$-texture and $m_{\mathrm{Re}\phi} = 500\,\mathrm{GeV}$. For other flavon masses, the bounds rescale approximately by $(m_{\mathrm{Re}\phi}/500\,\mathrm{GeV})^2$. The $\mu \leftrightarrow e$ conversion does not impose a significant bound in this case.

We find that the strongest constraint on the flavon mass and VEV for our texture is imposed by the $\mu \to e\gamma$ process. Figure 2 shows the allowed values of v_ϕ vs $m_{\mathrm{Re}\phi}$. As is clear from the above formulas, the bound scales approximately as $v_\phi \propto 1/m_{\mathrm{Re}\phi}$. We see that a flavon VEV as low as $100\,\mathrm{GeV}$ is allowed if $m_{\mathrm{Re}\phi} \sim 500\,\mathrm{GeV}$. And conversely, a light flavon with a mass smaller than $100\,\mathrm{GeV}$ is possible for $v_\phi > 1\,\mathrm{TeV}$. This mass range is certainly consistent with collider constraints since the production cross section for a leptophilic flavon is highly suppressed.

Finally, since the couplings of $\mathrm{Im}\phi$ are similar to those of $\mathrm{Re}\phi$, analogous bounds apply to the mass of $\mathrm{Im}\phi$.
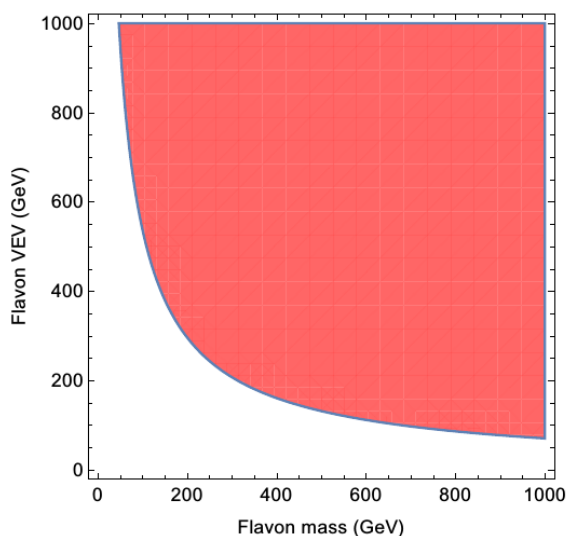
Figure 2. Allowed parameter space (shaded) for the texture at hand (eq. (A.1)) with negligible Higgs-flavon mixing. The strongest constraint is imposed by $\mathrm{BR}(\mu \to e\gamma)$.

3.2 Substantial Higgs-flavon mixing

The scalar mass eigenstates mediating LFV are H_1, H_2 and $\mathrm{Im}\phi$. The relevant interaction terms read

$$
\mathcal{L} \supset \left[\cos\theta \, \frac{Y_{ij}^{\mathrm{diag}}}{\sqrt{2}} + \sin\theta \, \widetilde{\kappa}_{ij}\right] \bar{l}_i P_R l_j \, H_1 + \left[-\sin\theta \, \frac{Y_{ij}^{\mathrm{diag}}}{\sqrt{2}} + \cos\theta \, \widetilde{\kappa}_{ij}\right] \bar{l}_i P_R l_j \, H_2
$$
$$
+ i\widetilde{\kappa}_{ij} \, \bar{l}_i P_R l_j \, \mathrm{Im}\phi + \mathrm{h.c.}
\tag{3.8}
$$

The couplings of H_1, H_2 to quarks are flavor-diagonal and obtained by rescaling the corresponding SM couplings with $\cos\theta$ and $-\sin\theta$, respectively.

Our previous tree and 1-loop level considerations can straightforwardly be generalized to the case at hand up to a trivial substitution of the lepton couplings and a summation over mass eigenstates. However, there are two significant changes. First, the $\mu \leftrightarrow e$ conversion is now possible at tree level. Second, the important new ingredient is a set of 2-loop Barr-Zee diagrams [42] with the top quark and the W in the loop (figure 3). Since both H_1 and H_2 have (flavor-diagonal) couplings to quarks, such diagrams make a significant contribution to $\mu \to e\gamma$.

We find again that the most important constraint on the flavon VEV for our texture comes from the $\mu \to e\gamma$ process. Let us consider it in more detail. The relevant amplitude is a sum of the 1- and 2-loop contributions,

$$
A_{\mu \to e\gamma}^L = A_{\mu \to e\gamma}^L(1-\mathrm{loop}) + A_{\mu \to e\gamma}^L(2-\mathrm{loop}) \ .
\tag{3.9}
$$

– 9 –
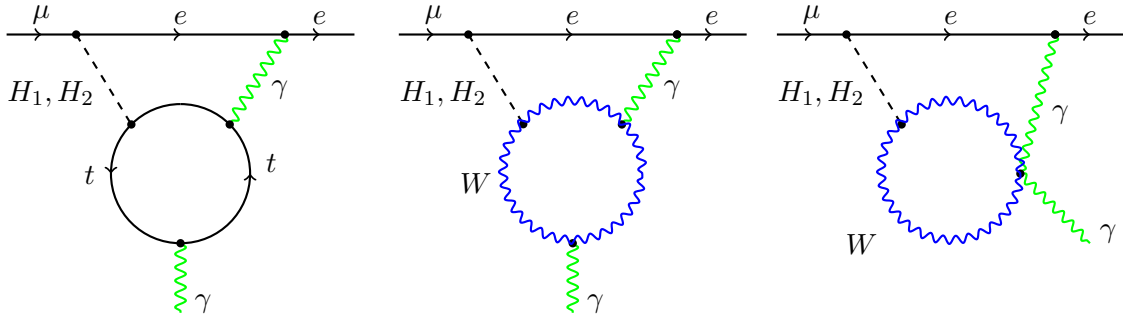
Figure 3. Barr-Zee diagrams contributing to $\mu \to e\gamma$.

At one loop we have

$$A^L_{\mu \to e\gamma}(1-\text{loop}) = -\frac{iem_\tau}{32\pi^2}\widetilde{\kappa}^*_{\tau e}\widetilde{\kappa}^*_{\mu\tau}\left\{\frac{\sin^2\theta}{m^2_{H_1}}\left[\frac{3}{2}-\log\left(\frac{m^2_{H_1}}{m^2_\tau}\right)\right]\right. \tag{3.10}$$

$$\left.+\frac{\cos^2\theta}{m^2_{H_2}}\left[\frac{3}{2}-\log\left(\frac{m^2_{H_2}}{m^2_\tau}\right)\right]-\frac{1}{m^2_{\text{Im}\phi}}\left[\frac{3}{2}-\log\left(\frac{m^2_{\text{Im}\phi}}{m^2_\tau}\right)\right]\right\}.$$

The 2-loop amplitude receives contributions from the top quark and the W boson [39],

$$A^L_{\mu \to e\gamma}(2-\text{loop}) = A^L_t + A^L_W, \tag{3.11}$$

with

$$A^L_t = -i\frac{e\alpha v G_F}{6\sqrt{2}\pi^3}\sin\theta\cos\theta\,\widetilde{\kappa}^*_{\mu e}\left[f(z_{tH_1})-f(z_{tH_2})\right]\,, \tag{3.12}$$

and

$$A^L_W = i\frac{e\alpha v G_F}{16\sqrt{2}\pi^3}\sin\theta\cos\theta\,\widetilde{\kappa}^*_{\mu e} \tag{3.13}$$

$$\times\left\{\left[3f(z_{WH_1})+5g(z_{WH_1})+\frac{3}{4}g(z_{WH_1})+\frac{3}{4}h(z_{WH_1})+\frac{f(z_{WH_1})-g(z_{WH_1})}{2z_{WH_1}}\right]\right.$$

$$\left.-\left[3f(z_{WH_2})+5g(z_{WH_2})+\frac{3}{4}g(z_{WH_2})+\frac{3}{4}h(z_{WH_2})+\frac{f(z_{WH_2})-g(z_{WH_2})}{2z_{WH_2}}\right]\right\}.$$

Here the loop functions are:

$$f(z) = \frac{1}{2}z\int_0^1 dx\frac{1-2x(1-x)}{x(1-x)-z}\log\left(\frac{x(1-x)}{z}\right), \tag{3.14}$$

$$g(z) = \frac{1}{2}z\int_0^1 dx\frac{1}{x(1-x)-z}\log\left(\frac{x(1-x)}{z}\right), \tag{3.15}$$

$$h(z) = z^2\frac{\partial}{\partial z}\left(\frac{g(z)}{z}\right) = \frac{z}{2}\int_0^1\frac{dx}{z-x(1-x)}\left[1+\frac{z}{z-x(1-x)}\log\left(\frac{x(1-x)}{z}\right)\right]. \tag{3.16}$$
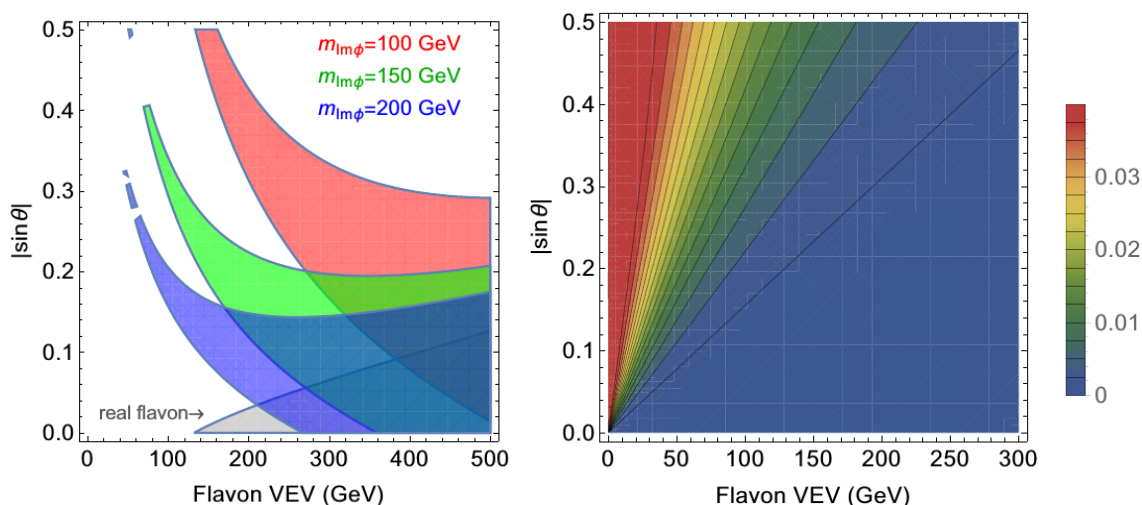
Figure 4. Left: parameter space allowed by the LFV constraints for $m_{\mathrm{Im}\phi} = 100, 150, 200 \, \mathrm{GeV}$. We have set $m_{H_2} = 500 \, \mathrm{GeV}$. (The discontinuities appear for technical reasons.) Right: $\mathrm{BR}_{\mathrm{eff}}(H_1 \to \mu\tau)$ as a function of v_ϕ and $|\sin\theta|$.

The arguments of these functions are defined by $z_{tH_i} = m_t^2/m_{H_i}^2$ and $z_{WH_i} = m_W^2/m_{H_i}^2$, with $i = 1, 2$. The $A_{\mu \to e\gamma}^R(2 - \mathrm{loop})$ amplitude is obtained by replacing $\widetilde{\kappa}_{ji}^*$ with $\widetilde{\kappa}_{ij}$. An analogous Z-boson contribution is suppressed compared to the photon one and therefore neglected. The resulting $\mu \to e\gamma$ decay rate is calculated according to

$$\Gamma(\mu \to e\gamma) = \frac{m_\mu^3}{4\pi} \left(|A^L|^2 + |A^R|^2 \right) . \tag{3.17}$$

Our results are presented in figure 4 (left). The shaded areas in the $(v_\phi, \sin\theta)$ plane are allowed by all the LFV constraints (of which $\mathrm{BR}(\mu \to e\gamma)$ is the strongest one) for a given m_{H_2} and $m_{\mathrm{Im}\phi}$. Comparison to the real flavon case shows that considerable cancellations between the H_i and $\mathrm{Im}\phi$ contributions take place. These are due to the pseudoscalar nature of $\mathrm{Im}\phi$ which introduces a relative minus sign and the lightness of $\mathrm{Im}\phi$ naturally expected in our framework. Similar cancellations apply also to the loop contribution for the $\mu \to eee$ process, while the $\mu \to e$ conversion bound is weaker even though it's not subject to the cancellations.

We see that the flavon VEV is allowed to be as low as $100 \, \mathrm{GeV}$ and a substantial Higgs-flavon mixing is consistent with the LFV data. The latter is also constrained by the collider and electroweak measurements as a function of m_{H_2} [33]. In particular, $|\sin\theta| \simeq 0.3$ is allowed for $m_{H_2} = 500 \, \mathrm{GeV}$. Figure 4 shows that this value is consistent with $v_\phi \sim 100 \, \mathrm{GeV}$ for a range of $m_{\mathrm{Im}\phi}$ around 150-200 GeV. As mentioned before, direct collider constraints on $\mathrm{Im}\phi$ are very loose due to its small couplings to leptons. Therefore, all of the relevant constraints are satisfied in that region. The right panel of figure 4 then shows that one expects a substantial decay rate $H_1 \to \mu\tau$, which we examine closely in the next section.

– 11 –

4 Leptonic Higgs decays

Our ultimate goal is to understand whether it is possible to obtain $\mathrm{BR}(H_1 \to \mu\tau)$ around 1% in our simple leptonic Froggatt-Nielsen framework. The SM Higgs decay into tau's has a branching fraction of 6%. Lepton flavor violating H_1 couplings are proportional to $|\sin\theta|$ which cannot be greater than 0.35 or so, resulting already in an order of magnitude suppression. This makes it clear that $\widetilde{\kappa}_{\mu\tau}$ and/or $\widetilde{\kappa}_{\tau\mu}$ must be comparable to or larger than the Higgs-tau Yukawa coupling in the Standard Model. This can be achieved in the Froggatt-Nielsen framework, yet it leads to the enhancement of the diagonal couplings as well. Since these are constrained by the LHC data, it is a non-trivial task to find a consistent model. One way to relieve the tension is to choose $\sin\theta < 0$ which leads to some cancellations in $H_1 \to l_i l_i$ for our Yukawa texture.

We find

$$\Gamma(H_1 \to \mu\tau) = \frac{m_{H_1}}{8\pi} \sin^2\theta \, \left(|\widetilde{\kappa}_{\mu\tau}|^2 + |\widetilde{\kappa}_{\tau\mu}|^2\right) \tag{4.1}$$

and

$$\Gamma(H_1 \to \tau\tau) = \frac{m_{H_1}}{8\pi} \left[\cos\theta \, \frac{Y_\tau^{\mathrm{diag}}}{\sqrt{2}} + \sin\theta \, \widetilde{\kappa}_{\tau\tau}\right]^2 , \tag{4.2}$$

and analogously for $H_1 \to \mu\mu$. We see that, in our convention, negative θ reduces $\Gamma(H_1 \to \tau\tau)$ without affecting the LFV rates.

The LHC experimental bounds on Higgs decays into leptons assume that the Higgs production cross section is not modified by new physics. This is not the case in our model since both the H_1 production cross section and its total width are reduced by the factor $\cos^2\theta$. Hence, the experimental limits in fact constrain the combination $\sigma(H_1)\,\mathrm{BR}(H_1 \to l_i l_j)$, which we take into account below.

The LHC searches for the Higgs decay into tau's yield [43–45]

$$\sigma(H_1)\,\mathrm{BR}(H_1 \to \tau\tau)_{\mathrm{ATLAS}} = \left(1.43^{+0.43}_{-0.37}\right) \times \sigma(h)\,\mathrm{BR}(h \to \tau\tau)_{\mathrm{SM}} ,$$
$$\sigma(H_1)\,\mathrm{BR}(H_1 \to \tau\tau)_{\mathrm{CMS}} = (0.91 \pm 0.28) \times \sigma(h)\,\mathrm{BR}(h \to \tau\tau)_{\mathrm{SM}} , \tag{4.3}$$

where σ is the production cross section and $\mathrm{BR}(h \to \tau\tau)_{\mathrm{SM}} = 0.063$. Combining these results naively gives approximately $\sigma(H_1)\,\mathrm{BR}(H_1 \to \tau\tau) = (1.06 \pm 0.23) \times \sigma(h)\,\mathrm{BR}(h \to \tau\tau)_{\mathrm{SM}}$, which we will use as the "guideline" bound. This implies that at 95% CL the tau coupling can be enhanced by no more than 25% or so, if the production cross section is the same as that in the SM. Another important constraint comes from the ATLAS limit on the Higgs decay into muons [46],

$$\sigma(H_1)\,\mathrm{BR}(H_1 \to \mu\mu) < 1.5 \times 10^{-3}\,\sigma(h) , \tag{4.4}$$

whereas the SM prediction is for $\mathrm{BR}(h \to \mu\mu)$ is 2×10^{-4}. This allows for the Higgs-muon coupling enhancement by a factor of 2.6 or so, again assuming the SM production cross section.
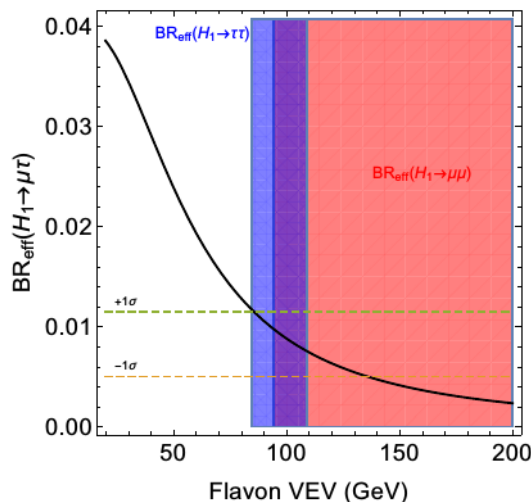
Figure 5. $\mathrm{BR}_{\mathrm{eff}}(H_1 \to \mu\tau)$ vs v_ϕ (black curve) for $\sin\theta = -0.3$. The red region is allowed by $\mathrm{BR}_{\mathrm{eff}}(H_1 \to \mu\mu)$ at 95% CL, the blue region is allowed by $\mathrm{BR}_{\mathrm{eff}}(H_1 \to \tau\tau)$, while their overlap (purple) is consistent with both. The dashed lines show the $\pm 1\sigma$ limits on the observed $\mathrm{BR}_{\mathrm{eff}}(H_1 \to \mu\tau)$.

To incorporate the difference between the H_1 and h production cross sections, we find it convenient to introduce the effective branching ratio $\mathrm{BR}_{\mathrm{eff}}(H_1 \to l_i l_j)$ through

$$\sigma(H_1)\,\mathrm{BR}(H_1 \to l_i l_j) = \sigma(h)\,\frac{\Gamma(H_1 \to l_i l_j)}{\Gamma_{\mathrm{SM}}^{\mathrm{total}}(h)} \equiv \sigma(h)\,\mathrm{BR}_{\mathrm{eff}}(H_1 \to l_i l_j)\,, \qquad (4.5)$$

where the first equality holds up to percent-level corrections and $\Gamma_{\mathrm{SM}}^{\mathrm{total}}(h) = 4.1\,\mathrm{MeV}$. The LHC result (1.1) then applies to this effective branching ratio.

Figure 5 shows that all of the constraints can be satisfied and the observed $\mathrm{BR}_{\mathrm{eff}}(H_1 \to \mu\tau)$ accommodated for $\sin\theta = -0.3$. This limits the flavon VEV to be around $100\,\mathrm{GeV}$, where partial cancellations between the SM Yukawa coupling and the $\widetilde{\kappa}$-contribution to $H_1 \to \tau\tau$ are effective.[6] The maximal allowed $\mathrm{BR}_{\mathrm{eff}}(H_1 \to \mu\tau)$ is close to 1% for this example. Note that $\mathrm{BR}_{\mathrm{eff}}(H_1 \to l_i l_j)$ is independent of $m_{\mathrm{Im}\phi}$ and m_{H_2} to leading order, so the latter can be adjusted in order to make a particular value of v_ϕ consistent with the LFV constraints.

The range of allowed $|\sin\theta|$ is limited by two factors: values substantially above 0.3 are inconsistent with the latest Higgs coupling data [47] according to which

$$|\sin\theta| < 0.33\,. \qquad (4.6)$$

At large m_{H_2} this bound is superseded by that from the electroweak precision measurements [33]. Values of $|\sin\theta|$ below 0.2 would require a low new physics scale $\Lambda \sim v_\phi/\epsilon$ in order to accommodate the observed $\mathrm{BR}_{\mathrm{eff}}(H_1 \to \mu\tau)$ (figure 4, right). For instance, at $\sin\theta = -0.2$, further new physics states are expected to appear at $\Lambda \sim 700\,\mathrm{GeV}$, whereas

---

[6]Large values $v_\phi > 700\,\mathrm{GeV}$ are also allowed by $\mathrm{BR}_{\mathrm{eff}}(H_1 \to \tau\tau)$. These however lead to negligible $\mathrm{BR}_{\mathrm{eff}}(H_1 \to \mu\tau)$.

for $\sin\theta = -0.1$ it becomes as low as $300\,\text{GeV}$. Whether such scenarios can be considered realistic depends on the details of the UV completion. While the flavor physics and collider bounds are highly model dependent, constraints on the multiplicity of states with electroweak quantum numbers are rather weak [48]. All in all, here we make the assumption that Λ around $1\,\text{TeV}$ can be consistent with the data in some classes of UV completions.

One should keep in mind the limitations of the present approach. Our effective Froggatt-Nielsen theory includes only $\text{Im}\phi$ and H_2 as additional active degrees of freedom. Concrete UV completions would involve further states which can affect our considerations, in particular the loop processes. Hence the LFV bounds we obtain should be treated as "guidelines". Also, within the effective theory one cannot explain why $m_{\text{Im}\phi}$ is comparable to v_ϕ, whereas one would naively expect it to be substantially lighter. This issue can presumably be addressed in more sophisticated UV completions, where $m_{\text{Im}\phi}$ is generated through a flavor-blind field.

Nevertheless, we find it encouraging that our simple framework can accommodate all the constraints and fit the observed $\text{BR}_{\text{eff}}(H_1 \to \mu\tau)$. The key ingredients are a texture with a large $\mu - \tau$ mixing and a leptophilic flavon with an electroweak size VEV. Surprisingly, such a set-up is rather poorly constrained, especially what concerns properties of $\text{Im}\phi$. Since it does not mix with the SM Higgs and couples only to leptons, the best limits would presumably come from exotic Z decays into 4 τ's. However, the rate is suppressed by the tau Yukawa coupling squared which makes it too small to place a useful bound on $m_{\text{Im}\phi}$.

5 Conclusion

Motivated by the tentative observation of the $h \to \mu\tau$ decay at the LHC, we have explored a lepton-specific Froggatt-Nielsen framework which naturally leads to lepton flavor violation at the observable level. The corresponding flavon mixes with the Standard Model Higgs such that the resulting Higgs-like boson decays to $\mu\tau$ with the branching ratio at the percent level.

This scenario necessitates a flavon VEV at the electroweak scale which we find to be consistent with the LFV and Higgs data constraints. The Froggatt-Nielsen symmetry must be either discrete or softly broken to allow for a massive $\text{Im}\phi$. Due to its pseudoscalar nature, the latter facilitates substantial cancellations in LFV processes and is only weakly constrained by collider data.

In this work, we have focused on a specific Yukawa texture resulting in a large mixing in the μ–τ sector. Further possible charge assignments as well as correlations among observables will be analyzed in our subsequent publication.

Acknowledgments

A Exact Yukawa matrix

The eigenvalues of the Yukawa matrix are sensitive to the exact values of the proportionality coefficients, which we provide below.

$$Y = \begin{pmatrix} 3.3855\ \epsilon^6 & -0.625\ \epsilon^6 & 3.5\ \epsilon^7 \\ 5.36\ \epsilon^4 & 6.1465\ \epsilon^4 & -3.125\ \epsilon^5 \\ 0.5\ \epsilon^2 & 0.5\ \epsilon^2 & 7.3312\ \epsilon^3 \end{pmatrix}, \tag{A.1}$$

where $\epsilon = 0.1$. One can verify that this matrix reproduces the observed lepton masses. It is diagonalized by the unitary transformations U_L and U_R as

$$Y_{\mathrm{diag}} = U_L Y U_R^\dagger, \tag{A.2}$$

with

$$U_L \approx \begin{pmatrix} 1 & -1 \times 10^{-3} & -8 \times 10^{-5} \\ -1 \times 10^{-3} & -1 & 5 \times 10^{-2} \\ -2 \times 10^{-4} & -5 \times 10^{-2} & -1 \end{pmatrix} \ \text{and} \ U_R \approx \begin{pmatrix} 0.8 & -0.7 & -6 \times 10^{-2} \\ -0.4 & -0.6 & 0.7 \\ -0.5 & -0.5 & -0.7 \end{pmatrix}.$$

We see that while U_L is approximately diagonal, U_R involves large angle rotations and is of "democratic" form. This is the key ingredient in obtaining a significant $\mathrm{BR}(H_1 \to \mu\tau)$.

References

[1] C.D. Froggatt and H.B. Nielsen, *Hierarchy of Quark Masses, Cabibbo Angles and CP-violation*, *Nucl. Phys.* **B 147** (1979) 277 [INSPIRE].

[2] CMS collaboration, *Search for Lepton-Flavour-Violating Decays of the Higgs Boson*, *Phys. Lett.* **B 749** (2015) 337 [arXiv:1502.07400] [INSPIRE].

[3] ATLAS collaboration, *Search for lepton-flavour-violating $H \to \mu\tau$ decays of the Higgs boson with the ATLAS detector*, *JHEP* **11** (2015) 211 [arXiv:1508.03372] [INSPIRE].

[4] V. Silveira and A. Zee, *Scalar phantoms*, *Phys. Lett.* **B 161** (1985) 136 [INSPIRE].

[5] R. Schabinger and J.D. Wells, *A minimal spontaneously broken hidden sector and its impact on Higgs boson physics at the large hadron collider*, *Phys. Rev.* **D 72** (2005) 093007 [hep-ph/0509209] [INSPIRE].

[6] B. Patt and F. Wilczek, *Higgs-field portal into hidden sectors*, hep-ph/0605188 [INSPIRE].

[7] K.S. Babu and S. Nandi, *Natural fermion mass hierarchy and new signals for the Higgs boson*, *Phys. Rev.* **D 62** (2000) 033002 [hep-ph/9907213] [INSPIRE].

[8] G.F. Giudice and O. Lebedev, *Higgs-dependent Yukawa couplings*, *Phys. Lett.* **B 665** (2008) 79 [arXiv:0804.1753] [INSPIRE].

[9] M. Bauer, M. Carena and K. Gemmler, *Flavor from the Electroweak Scale*, *JHEP* **11** (2015) 016 [arXiv:1506.01719] [INSPIRE].

[10] A. Goudelis, O. Lebedev and J.-h. Park, *Higgs-induced lepton flavor violation*, *Phys. Lett.* **B 707** (2012) 369 [arXiv:1111.1715] [INSPIRE].

[11] G. Blankenburg, J. Ellis and G. Isidori, *Flavour-Changing Decays of a 125 GeV Higgs-like Particle*, *Phys. Lett.* **B 712** (2012) 386 [arXiv:1202.5704] [INSPIRE].

[12] D. McKeen, M. Pospelov and A. Ritz, *Modified Higgs branching ratios versus CP and lepton flavor violation*, *Phys. Rev.* **D 86** (2012) 113004 [arXiv:1208.4597] [INSPIRE].

[13] S. Davidson and P. Verdier, *LHC sensitivity to the decay $h \to \tau^{\pm} mu^{\mp}$*, *Phys. Rev.* **D 86** (2012) 111701 [arXiv:1211.1248] [INSPIRE].

[14] A. Dery, A. Efrati, Y. Hochberg and Y. Nir, *What if $BR(h \to \mu\mu)/BR(h \to \tau\tau)$ does not equal m_{μ}^2/m_{τ}^2?*, *JHEP* **05** (2013) 039 [arXiv:1302.3229] [INSPIRE].

[15] M. Arroyo, J.L. Diaz-Cruz, E. Diaz and J.A. Orduz-Ducuara, *Flavor Violating Higgs signals in the Texturized Two-Higgs Doublet Model (2HDM-Tx)*, arXiv:1306.2343 [INSPIRE].

[16] A. Crivellin, S. Najjari and J. Rosiek, *Lepton Flavor Violation in the Standard Model with general Dimension-Six Operators*, *JHEP* **04** (2014) 167 [arXiv:1312.0634] [INSPIRE].

[17] A. Crivellin, M. Hoferichter and M. Procura, *Improved predictions for $\mu \to e$ conversion in nuclei and Higgs-induced lepton flavor violation*, *Phys. Rev.* **D 89** (2014) 093024 [arXiv:1404.7134] [INSPIRE].

[18] J. Kopp and M. Nardecchia, *Flavor and CP-violation in Higgs decays*, *JHEP* **10** (2014) 156 [arXiv:1406.5303] [INSPIRE].

[19] A. Dery, A. Efrati, Y. Nir, Y. Soreq and V. Susič, *Model building for flavor changing Higgs couplings*, *Phys. Rev.* **D 90** (2014) 115022 [arXiv:1408.1371] [INSPIRE].

[20] D. Aristizabal Sierra and A. Vicente, *Explaining the CMS Higgs flavor violating decay excess*, *Phys. Rev.* **D 90** (2014) 115004 [arXiv:1409.7690] [INSPIRE].

[21] L. de Lima, C.S. Machado, R.D. Matheus and L.A.F. do Prado, *Higgs Flavor Violation as a Signal to Discriminate Models*, *JHEP* **11** (2015) 074 [arXiv:1501.06923] [INSPIRE].

[22] I. Doršner, S. Fajfer, A. Greljo, J.F. Kamenik, N. Košnik and I. Nišandžic, *New Physics Models Facing Lepton Flavor Violating Higgs Decays at the Percent Level*, *JHEP* **06** (2015) 108 [arXiv:1502.07784] [INSPIRE].

[23] T. Goto, R. Kitano and S. Mori, *Lepton flavor violating Z-boson couplings from nonstandard Higgs interactions*, *Phys. Rev.* **D 92** (2015) 075021 [arXiv:1507.03234] [INSPIRE].

[24] X.-G. He, J. Tandean and Y.-J. Zheng, *Higgs decay $h \to \mu\tau$ with minimal flavor violation*, *JHEP* **09** (2015) 093 [arXiv:1507.02673] [INSPIRE].

[25] W. Altmannshofer, S. Gori, A.L. Kagan, L. Silvestrini and J. Zupan, *Uncovering Mass Generation Through Higgs Flavor Violation*, *Phys. Rev.* **D 93** (2016) 031301 [arXiv:1507.07927] [INSPIRE].

[26] F. Feruglio, P. Paradisi and A. Pattori, *Lepton Flavour Violation in Composite Higgs Models*, *Eur. Phys. J.* **C 75** (2015) 579 [arXiv:1509.03241] [INSPIRE].

[27] N. Bizot, S. Davidson, M. Frigerio and J.L. Kneur, *Two Higgs doublets to explain the excesses $pp \to \gamma\gamma(750 \,\text{GeV})$ and $h \to \tau^{\pm}\mu^{\mp}$*, *JHEP* **03** (2016) 073 [arXiv:1512.08508] [INSPIRE].

[28] M. Buschmann, J. Kopp, J. Liu and X.-P. Wang, *New Signatures of Flavor Violating Higgs Couplings*, arXiv:1601.02616 [INSPIRE].

[29] F.J. Botella, G.C. Branco, M.N. Rebelo and J.I. Silva-Marcos, *What if the Masses of the First Two Quark Families are not Generated by the Standard Higgs?*, arXiv:1602.08011 [INSPIRE].

[30] H. Bélusca-Maïto and A. Falkowski, *On the exotic Higgs decays in effective field theory,* arXiv:1602.02645 [InSPIRE].

[31] W. Buchmüller, K. Hamaguchi, O. Lebedev, S. Ramos-Sanchez and M. Ratz, *Seesaw neutrinos from the heterotic string, Phys. Rev. Lett.* **99** (2007) 021601 [hep-ph/0703078] [InSPIRE].

[32] O. Lebedev and H.M. Lee, *Higgs Portal Inflation, Eur. Phys. J.* **C 71** (2011) 1821 [arXiv:1105.2284] [InSPIRE].

[33] A. Falkowski, C. Gross and O. Lebedev, *A second Higgs from the Higgs portal, JHEP* **05** (2015) 057 [arXiv:1502.01361] [InSPIRE].

[34] SINDRUM collaboration, U. Bellgardt et al., *Search for the Decay $\mu^+ \to e^+e^+e^-$, Nucl. Phys.* **B 299** (1988) 1 [InSPIRE].

[35] HEAVY FLAVOR AVERAGING GROUP collaboration, Y. Amhis et al., *Averages of B-Hadron, C-Hadron and tau-lepton properties as of early 2012,* arXiv:1207.1158 [InSPIRE].

[36] K. Hayasaka et al., *Search for Lepton Flavor Violating Tau Decays into Three Leptons with 719 Million Produced $\tau^+\tau^-$ Pairs, Phys. Lett.* **B 687** (2010) 139 [arXiv:1001.3221] [InSPIRE].

[37] MEG collaboration, J. Adam et al., *New constraint on the existence of the $\mu^+ \to e^+\gamma$ decay, Phys. Rev. Lett.* **110** (2013) 201801 [arXiv:1303.0754] [InSPIRE].

[38] SINDRUM II collaboration, W.H. Bertl et al., *A Search for muon to electron conversion in muonic gold, Eur. Phys. J.* **C 47** (2006) 337 [InSPIRE].

[39] R. Harnik, J. Kopp and J. Zupan, *Flavor Violating Higgs Decays, JHEP* **03** (2013) 026 [arXiv:1209.1397] [InSPIRE].

[40] R. Kitano, M. Koike and Y. Okada, *Detailed calculation of lepton flavor violating muon electron conversion rate for various nuclei, Phys. Rev.* **D 66** (2002) 096002 [*Erratum ibid.* **D 76** (2007) 059902] [hep-ph/0203110] [InSPIRE].

[41] R. Alonso, M. Dhen, M.B. Gavela and T. Hambye, *Muon conversion to electron in nuclei in type-I seesaw models, JHEP* **01** (2013) 118 [arXiv:1209.2679] [InSPIRE].

[42] S.M. Barr and A. Zee, *Electric Dipole Moment of the Electron and of the Neutron, Phys. Rev. Lett.* **65** (1990) 21 [*Erratum ibid.* **65** (1990) 2920] [InSPIRE].

[43] ATLAS collaboration, *Evidence for the Higgs-boson Yukawa coupling to tau leptons with the ATLAS detector, JHEP* **04** (2015) 117 [arXiv:1501.04943] [InSPIRE].

[44] CMS collaboration, *Precise determination of the mass of the Higgs boson and tests of compatibility of its couplings with the standard model predictions using proton collisions at 7 and 8 TeV, Eur. Phys. J.* **C 75** (2015) 212 [arXiv:1412.8662] [InSPIRE].

[45] CMS collaboration, *Evidence for the 125 GeV Higgs boson decaying to a pair of τ leptons, JHEP* **05** (2014) 104 [arXiv:1401.5041] [InSPIRE].

[46] ATLAS collaboration, *Search for the Standard Model Higgs boson decay to $\mu^+\mu^-$ with the ATLAS detector, Phys. Lett.* **B 738** (2014) 68 [arXiv:1406.7663] [InSPIRE].

[47] ATLAS and CMS Collaborations, *Measurements of the Higgs boson production and decay rates and constraints on its couplings from a combined ATLAS and CMS analysis of the LHC pp collision data at $\sqrt{s} = 7$ and 8 TeV,* ATLAS-CONF-2015-044 (2015).

[48] C. Gross, O. Lebedev and J.M. No, *Drell-Yan Constraints on New Electroweak States and the Di-photon Anomaly,* arXiv:1602.03877 [InSPIRE].